Study of the structure and phase composition of a quasi-high-entropy alloy of the Cr–Mn–Ni–Fe–Co–Nb system

V. Yu. Kulikov, *Cand. Eng., Prof.* [1], *e-mail: mlpikm@mail.ru;*
Sv. S. Kvon, *Cand. Eng., Prof.* [1], *e-mail: svetlana.1311@mail.ru;*
A. Z. Isagulov, *Dr. Eng., Prof.* [1], *e-mail: isagulov_aristotel@kstu.kz;*
S. K. Arinova, *Ph. D., Lecturer* [1], *e-mail: sanya_kazah@mail.ru*

[1] *Karaganda Technical University (Karaganda, Kazakhstan)*

The paper presents the results of studying the structure and properties of quasi-high-entropy alloys (QHEAs) of the Cr–Mn–Ni–Fe–Co–Nb system, with the Nb content 0–18 %. These alloys were smelted with partial use of ferroalloys in the charge, which is their feature and determines formation of new phases. For the experimental alloys obtained under the specified smelting conditions and charge composition, the Laves phase and the σ phase were not detected. The structure of the studied alloys is represented by the FCC solid solution that includes all the metals, and the niobium content varies widely. In addition, the structure is represented by interstitial phases: niobium carbide $NbC_{0.76-1.0}$, manganese carbide Mn_7C_3 and intermetallic CrNi with the cubic lattice. Introduction of niobium in the Cr–Mn–Ni–Fe–Co–Nb system in the amount of 14–16 % leads to increase of hardness, compression strength and wear resistance. The niobium content above 18 % leads to a slight decrease of these parameters, which can be explained by its uneven distribution in the structure. The study shows that the partial use of ferroalloys in the charge makes it possible to obtain alloys of the Cr–Mn–Ni–Fe–Co–Nb system of the QHEA type that have a higher commercial attractiveness due to simplification of the smelting technology and the cost of the charge.

Key words: quasi-high-entropy alloys, Cr–Mn–Ni–Fe–Co–Nb system, ferroalloys, structure, hardness, wear resistance, carbides, intermetallic compounds.
DOI: 10.17580/cisisr.2025.01.08

Introduction

The alloys of the Cr–Mn–Ni–Fe–Co–Nb system, which composition was developed on the base of an entropy approach, are the objects of this research. Such alloys are named as high-entropy alloys (HEAs). Their main feature is absence of a dominating element in composition, e.g. Fe in steel. At least 5 elements should be presented in HEA composition, and content of the elements in the first HEAs should be in equiatomic concentration [1–7]. Additional development of HEAs provided widening of the boundaries of composition understanding, i.e. content of the elements in the alloy composition can be characterized by relation differing from an equiatomic one; however, absence of a dominating element in the composition still remains the main HEA feature. Such approach in alloy creation provides high mixing entropy of the alloy, which leads to essential improvement of properties in comparison of the steels of the same use, for example.

High requirements to charge materials and smelting conditions are considered as other HEA features; all high-entropy alloys are smelted from high clean metals with attraction of definite smelting technologies: plasma synthesis, multiple remelting, smelting in vacuum or in protection medium etc [6, 8–12].

It is evident that these requirements ensure high cost and restrict industrial use, despite demonstration of high operating properties.

At present time, the alloys on the base of transition metals are most widely distributed and, respectively, most examined. The first HEA (Cantor alloy) was suggested on the base of Cr–Mn–Ni–Fe–Co system [1], where all elements initially have equiatomic concentration.

The properties of this system were improved consequently via addition of such elements as Ti, Nb, Mo, V, Al, Cu [13–18], as well as C and B [19, 20].

Essential amount of researches [20–25] was devoted to examination of niobium effect on the alloy properties. Positive niobium effect on such properties as bending strength, hardness, wear resistance are noted in these researches. Improvement of mechanical properties are connected by the researchers with forming of Laves phase, which plays the role of hardening phase. The research [21] included investigation of the alloys, where niobium content varied within the range $x = 0.25–1.2$ for the Cr–Mn–Ni–Fe–Co–Nb system; it was noted that structure of these alloys is hypoeutectic, where eutectic consists of solid FCC solution and Laves phase, for niobium content up to $x = 0.45$ (what corresponds to 12.9 % (mass.)). When niobium content increases up to $x = 0.5$ (14.2 % (mass.)), the alloy structure is identified as eutectic one and then – hypereutectic one, with rise of strength properties and lowering of ductility. The same tendency in evolution of properties is observed in the research [22].

It should be also mentioned that uneven niobium distribution in composition of solid FCC solution is observed in all researches [21–25], i.e. the areas which are depleted or, on the contrary, enriched by niobium are presented.

Study of the structure of the alloy of the Cr–Mn–Ni–Fe–Co–Nb system, which was smelted with partial use of ferroalloys instead of clean metals, is the aim of this research. Use of ferroalloys instead of clean metals is just the main feature of this study in comparison with other works in this direction.

Use of ferroalloys in charge materials allows to simplify the smelting technology owing to decrease of smelting temperature for charge and to lower charge cost, because ferroalloys are more cheap than clean metals. These two circumstances allow to increase commercial attractiveness of final alloy and to promote its more side distribution in the industry.

Ferroalloys are not dual-component systems; in addition to the main components (ferrum, chromium, niobium, manganese etc.) they always contain impurities, such as carbon, silicon, sulfur, phosphorus etc.

Presence of additional elements in the Cr–Mn–Ni–Fe–Co–Nb system, other conditions of smelting and crystallization can lead to formation of other phases and structure differing from those described in the researches [21–25].

The alloys obtained with use of ferroalloys correspond to the principle of HEA creation, because they have no dominating element in their structure. However, the objects of this research were smelted in the conditions, which are different from the classic HEA conditions. They contain impurities, thereby it is more correct to name them quasi-high-entropy alloys (QHEAs), meaning pseudo-high-entropy alloys. Such term was already used in the researches [19, 26].

Materials and methods

Composition of the materials which were used as charge components are presented in the **Table 1**. Cobalt and nickel were introduced as pure metals of K1Au and N-1u grades respectively, they have the lowest melting temperature in comparison with the other elements of this system (1495 °C and 1455 °C). Manganese only in this system is characterized by lower temperature (1246 °C), but it was introduced in charge as ferromanganese, due to its acceptability. Other elements were introduced also as ferroalloys.

The grades of ferroalloys with the lowest carbon content were chosen from the existing ones. Charge composition was created in such way, that niobium content varied within the range 14–18 %, because just such concentration ensures the best combination of strength and ductility properties [22]. Other elements (Mn, Fe, Cr, Ni and Co) were characterized by approximately equal mass parts.

All charge components were ground in the Retch mill during 10 min, dispersity of these components was presented by 2–3 mm fraction for 90 %. Then charge mix was thoroughly mixed in a laboratorial Schatz mixer and then smelted in a graphite crucible of UIP-16 induction furnace with forced cooling system. To provide homogeneity of composition and to exclude external contamination, an obtained ingot with mass 4 kg was cast in a chemically inert corundum-mullite-zirconium (CMZ) crucible, then it was subjected to remelting and again to casting in a CMZ crucible. The samples for analysis were prepared after complete cooling of ingots. Structure, chemical and phase composition, hardness, compression strength and wear resistance were examined on experimental samples.

Chemical composition was determined using Poly Spec-F spectrometer.

Wear resistance testing was carried out in the Tribometer machine (manufactured by CSM Instruments, Switzerland) via the method of measuring slipping with the following conditions: path length 4 mm; applied load 1 N; velocity 5 cm/s; ball counterbody of WC–Co (VK6) with 3 mm diameter; road haul 20,000 cycles (160 m); air medium; preliminary processing of samples – ultrasonic cleaning (USC) in isopropyl alcohol. The presented wear resistance was evaluated by the results of wear groove parameters in a sample according to the formula

$$\varepsilon' = \frac{W}{A}$$

where W – volume of wear products, mm^3;

A – friction work, N·m.

Wear groove parameters for determination of volume of wear products were identified via optical profilometer WYKO NT1100. The results of tribological testing were processed automatically using Instrum X Tribometer software. Hardness determination was conducted via Willson 1150 device with measurements at least n 5 points. Tensile strength was determined in the testing machine INSTRON with 3 doubles.

Structure analysis was implemented using scanning electron microscope S-3400N, which is equipped by X-ray energy-dispersion spectrometer NORAN produced by Hitachi HighTechnologies Corporation.

X-ray investigations were conducted via diffractometer X'PertPRO with CuKα-radiation. Accelerated voltage was 30 kV, current – 10 mA, nickel filter was used. Diffraction spectrum was caught in the range of 5 to 120 Bragg degrees. Goniometer focusing was carried out in accordance with

Table 1. Composition of charge materials

Element, % / Material	Mn	Nb	Fe	Cr	Ni	Co	C	Si	P	S
FeMn80C05	75.1	–	25.2	–	–	–	≤ 0.1	1.85	≤ 0.3	≤ 0.03
FKh001A	–	–	32.04	68.2	–	–	≤ 0.01	0.82	≤ 0.02	≤ 0.02
FNb58	–	62	35.5	–	–	–	0.3	1.8	0.04	0.05
Ni N-1u	–	–	–	–	99.95	–	≤ 0.01	0.002	0.001	0.001
Co K1Au	0.03	–	0.2	–	–	99.3	0.02	–	0.003	0.004

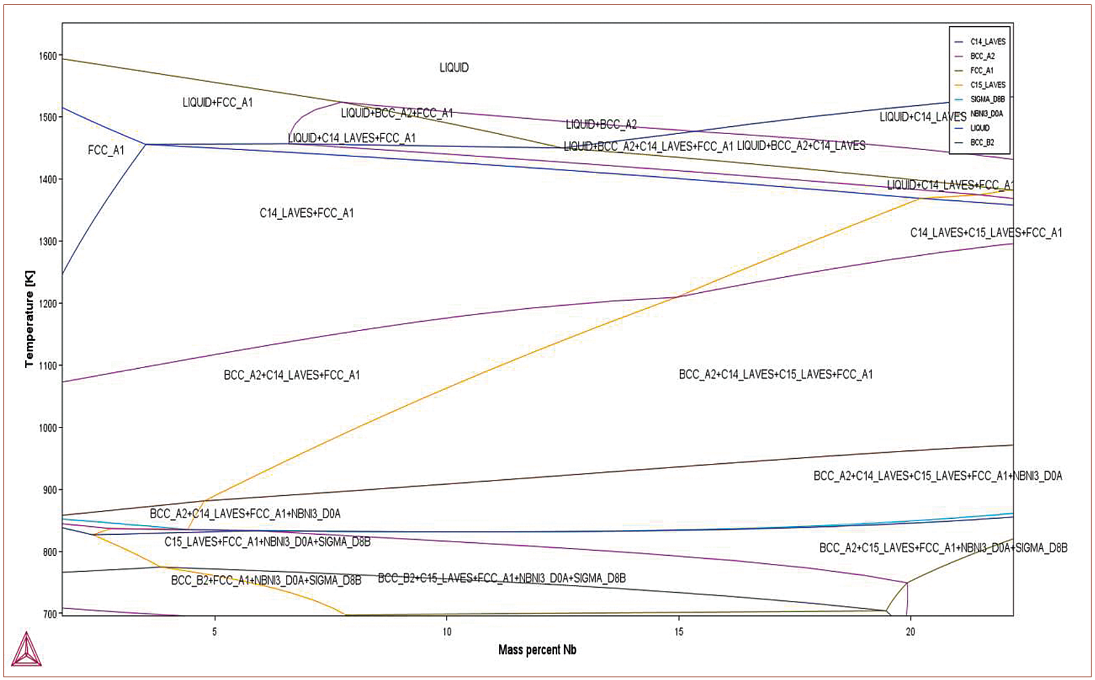

Fig. 1. Equilibrium diagram for alloys of the Cr–Mn–Ni–Fe–Co–Nb system, which is calculated ThermoCalc software

Bragg-Brentano. Processing of experimental spectra was conducted using software of a diffractometer X'Pert High Score Plusversion 2.2b and X'Pert High Score version 2.2b.

Results and discussion

Thermodynamic analysis of alloys on the base of the Cr–Mn–Ni–Fe–Co–Nb system, with different niobium content in this system, was preliminarily carried out with use of ThermoCalc software (version 2023b, database TCFE13).

It can be seen from the **Fig. 1** that presence of the following phases: mix of BCC+FCC solid solutions, Laves phase, intermetallic of $NbNi_3$ type and σ-phase, is possible in the alloys of the above-mentioned system, within the examined range of concentrations and with uniform cooling.

The structure presented by FCC solid solution of BCC+FCC mix is typical for the Cr–Mn–Ni–Fe–Co–Nb system, as it was noted in the researches [1, 3, 16, 22].

However, niobium introduction leads to forming of new phases, such as Laves phase and σ-phase, what definitely leads to variation of the alloy properties [22–26]. It is based on the calculation data that Laves phase as well as solid solutions can be presented by different compositions. Calculated composition of the phases, which are presented in the diagram, is shown in the **Table 2**.

It should be underlined that presence of carbon, sulfur, phosphorus and silicon, which will be presented in the final alloy due to their transition from charge, was not taken into account during calculation of this diagram. Carbon presence can evidently lead to forming of carbide phase, while silicon presence – to forming of silicates etc. In other words, the equilibrium diagram (presented in the Fig. 1) can differ essentially from the real formation process in the examined system.

Chemical composition, strength, hardness and wear resistance of the system were examined at the first stage, the results are displayed in the **Table 3** and **Table 4.**

Carbon and silicon are presented in all pilot samples, as it was awaited; traces of sulfur and phosphorus were also noted, but it was impossible to determine their exact amount.

It can be seen from the Table 4 that niobium content in the alloy has significant effect on all examined properties. Hardness, compression strength and wear resistance increase

Table 2. Calculation results for the phases presented in the diagram

Phases	Content, %					
	Nb	Fe	Cr	Ni	Mn	Co
C14_LAVES#1	41	24	16	7	6	6
FCC_A1#1 (ГЦК)	2	23	22	17	19	17
BCC_A2+C14_LAVES+FCC_A1+$NbNi_3$_D0A	0.4	26	21	16	18	17
BCC_A2#1 (ОЦК)	0.5	11	68	0.5	16	4
C14_LAVES#1	44	37	0.6	0.6	0.3	0.5
$NbNi_3$_D0A#1	34	0.3	0	63	0	0
Liquid+BCC_A2+C14_LAVES+FCC_A1	12	18	21	15	18	16
BCC_A2+C15_LAVES+FCC_A1+$NbNi_3$_D0A+SIGMA_D8B	18	12	21	15	18	16
`C15_LAVES	44	0.5	0.3	0.5	0	42

Table 3. Chemical composition of pilot alloys

Sample	Element, % (mass.)							
	Co	Cr	Fe	Ni	Mn	Nb	C	Si
1	19.8	19.2	20.8	19.28	19.8	0	0.25	0.009
2	16.94	16.82	18.5	16.73	16.53	14.23	0.23	0.002
3	16.78	16.54	17.88	16.72	16.28	15.51	0.25	0.002
4	16.58	16.60	17.54	16.34	16.32	16.33	0.28	0.002
5	16.67	16.86	14.60	16.49	16.60	18.45	0.32	0.0022

Table 4. The results of investigation of properties of pilot alloys

Sample	Hardness, HV	Compression strength, MPa	Friction coefficient	Wear groove width, µm	Reduced wear resistance, mm³/(N·m)
1	240	550	0.45	172.2	3.67 · 10–6
2	243	550	0.44	167. 4	3.24 · 10–6
3	282	630	0.42	146.8	2.92 · 10–6
4	395	720	0.39	145.4	1.88 · 10–6
5	367	632	0.43	178.3	3.04 · 10–6

with rise of niobium content, what well correlates with the data of the researches [19–25]. However, when niobium content exceeds 18 % (sample 5), all strength properties and wear resistance decrease and become comparative with the values of properties for the sample without niobium. This fact contradicts to the results, which were obtained earlier [21–25].

To explain this divergence and to assess a real phase composition in comparison with calculated composition (noted in the researches [21, 22]), phase composition and structure were examined (**Fig. 2** and **Fig. 3** respectively).

The results of X-ray phase analysis display that FCC solid solution is presented in all samples; it includes all metals dissolved, as well as niobium carbide of $NbC_{0.76-1.0}$ type, manganese carbide of Mn_7C_3 type and intermetallic of CrNi type with cubic lattice. In this research we could not identify the definite phases where silicon is presented, but chemical analysis has shown its presence. Probably silicon is included in composition of BCC solution, which presence is suggested according to thermodynamic calculations (see Fig. 1). However, these peaks were not registered in X-ray patterns, what perhaps can be connected with low content of BCC solution.

Structures of all alloys are presented at least by two phases (sample 1) and more than two phases (samples 2–5). To provide more detailed analysis of the structure, micro-X-ray-spectral analysis (MXSA) was carried out in different phase areas of pilot samples.

Chemical analysis in the selected points is presented in the **Table 5**.

It can be seen from the Table 4 that the sample 1 is presented by mix of two sold FCC solutions: one phase is enriched by Cr and other – by Ni. Silicon in small amount is also presented in the second phase, other phases were not identified. The second alloy contains 14.2 % (mass.) of niobium (based on the data of general analysis). MXSA shows essential oscillation by niobium – from 29.3 to 13.6 % (mass.).

The sample with total niobium content 15.5 % (mass.) is characterized by very large deviation of Nb content in different points. Solid FCC solution with various Nb content is presented in the points 1 and 2. Substantial silicon amount is also presented in these areas; it is evidently included in composition of a solid solution, because it is not extracted in a separate phase. The point 3 reflects non-metallic inclusion of oxide type, based on high content of niobium and oxygen. The point 4 is a solid solution on the base of ferrum and manganese presence in this point is not observed.

The sample 4 (niobium content 16.3 % (mass.)) is characterized by solid solution with various niobium content. Niobium content in the point 3 is maximal (27 %), with

Table 5. Chemical composition in several points of pilot samples

Sample	Area	Co	Cr	Fe	Ni	Mn	Nb	Si/O
1	1	13.3	53.6	19.2	4.3	9.6	0	0
	2	26.5	4.1	21.7	35.61	12.0	0	0.09
2	1	9.5	9.4	19.8	13.5	18.1	29.3	0.4
	2	11.9	17.8	20.42	19.2	17.0	13.6	0.08
3	1	9.1	5.9	18,6	14.9	19.2	28.2	4.2
	2	8.9	3.8	15.8	9.1	17.2	39.0	6.1
	3	–	–	–	–	–	96.8	–/3.2
	4	10.5	8.6	50.3	19.8	–	7.7	3.1
4	1	17.0	16.9	21.2	13.8	13.3	16.9	0.9
	2	13.6	18.9	23.1	15.3	15.45	13.63	0.02
	3	–	18.6	18.57	17.3	16.89	27.4	0.78
	4	16.6	14.89	22.2	23.6	11.06	16.44	0.21
5	1	18.2	16.9	18.78	15.6	11.2	19.24	0.08

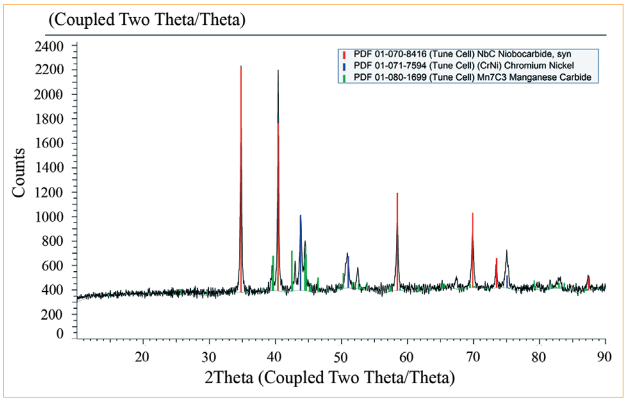

Sample 2

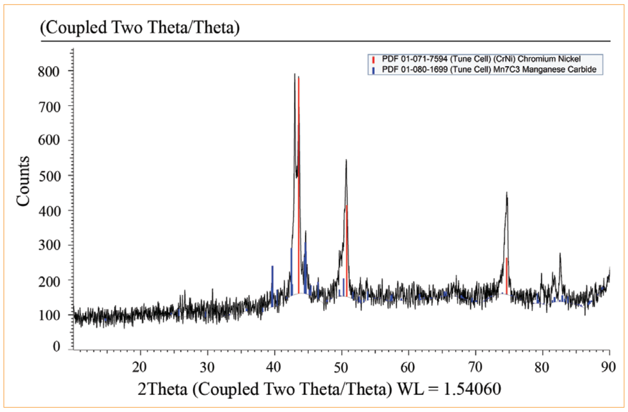

Sample 3

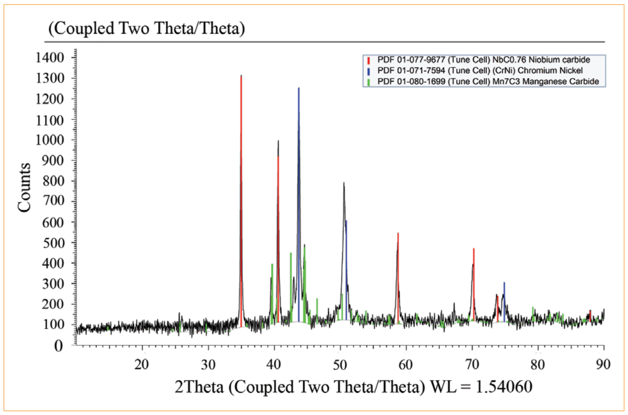

Sample 3

Fig. 2. The results of X-ray phase analysis for pilot samples with different niobium content

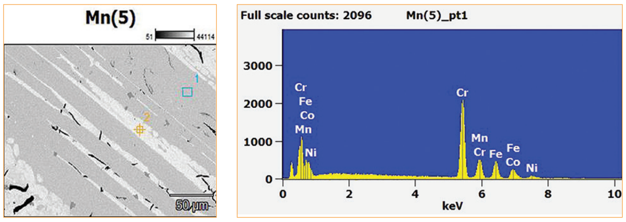

Sample 1

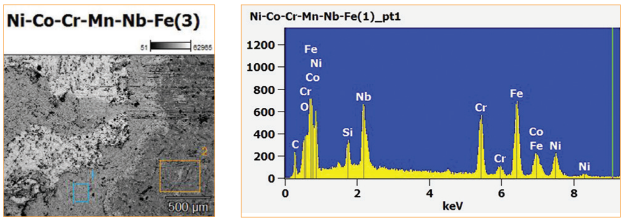

Sample 2

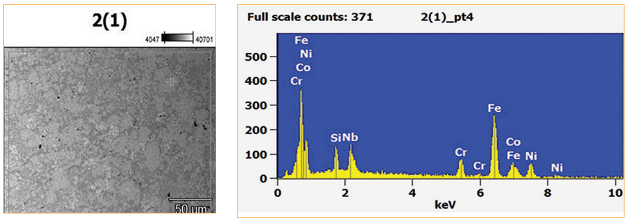

Sample 3

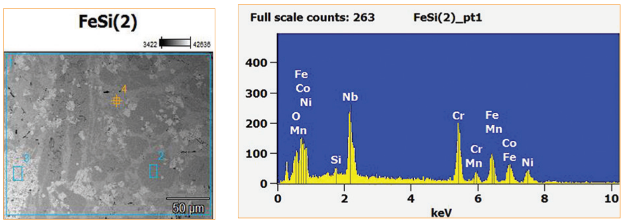

Sample 4

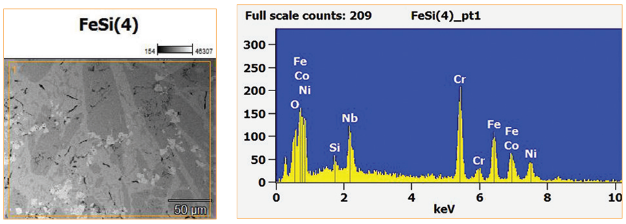

Sample 5

Fig. 3. Structure of pilot alloys

cobalt absence in this phase. Silicon is presented in all examined points, but it does not form any compound (as it was noted before) and evidently is included in composition of the solution.

The sample 5 (niobium content 18.45 % (mass.)) is also presented by solid solution with various niobium content. The point 1 displays niobium content 19.24 % (mass.), other phases contain lower niobium content (dark areas) or, on the contrary, they are excessively enriched by niobium (light grey areas).

It should be noted that rather essential heterogeneity of distribution of the elements is observed in the obtained alloys. It is especially clearly seen for the sample with the most high niobium content (sample 5).

The chart of elements distribution in the samples 2 and 5 is presented in the **Fig. 4**. While distribution features of all elements in the sample 2 are homogeneous, the sample 5 is characterized by evident inhomogeneity of distribution; especially it is related to niobium distribution, which is deposed along boundaries of the phases. It can be predicted that strength properties of this alloy will be not satisfactory.

If we shall compare the data of the Tables 4 and 2, we can suggest that the Laves phase was not observed in the examined alloys, despite the calculation data (see Fig. 1). Comparison of calculated composition of the Laves phase and

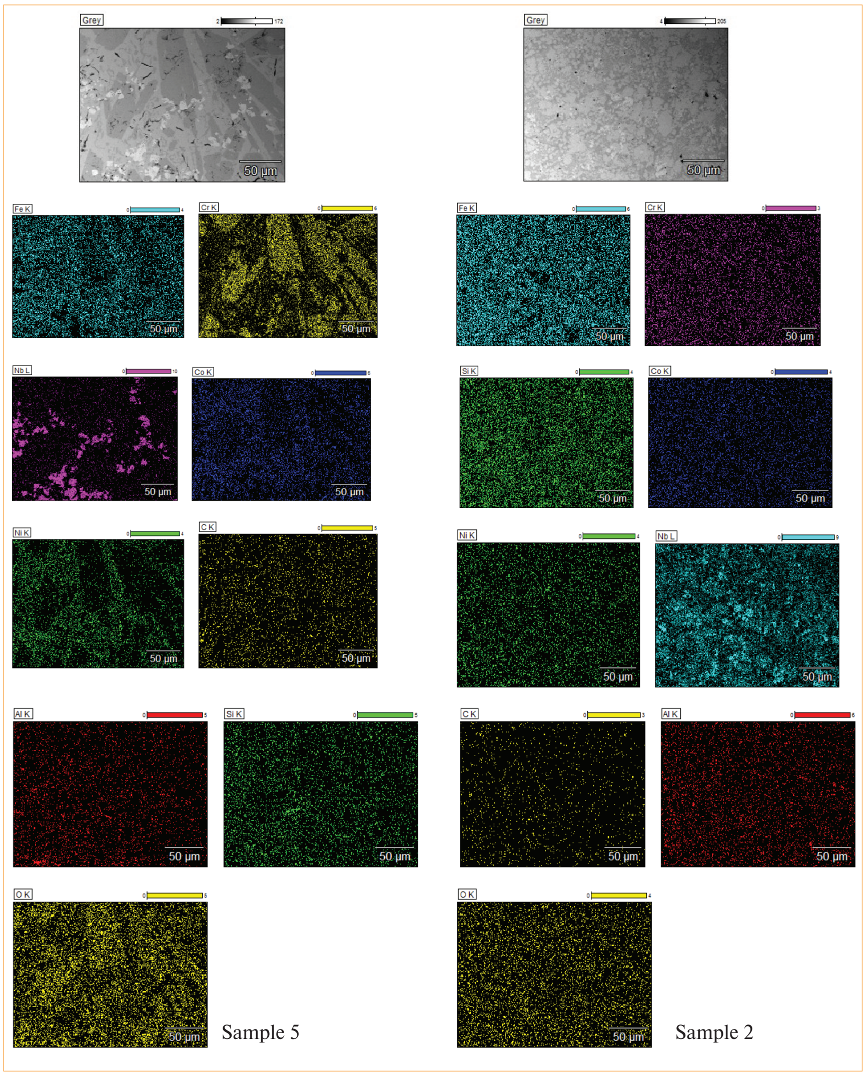

Fig. 4. The chart of elements distribution in the samples 2 and 5

composition obtained via MXSA did not display coincidences, what allows to propose that formation of the Laves phases is not realized practically in such crystallization conditions and for this composition of initial charge. However, interstitial phases, such as niobium carbide, manganese carbides and intermetallics of CrNi type, were observed in the structure of pilot alloys (see Fig. 2).

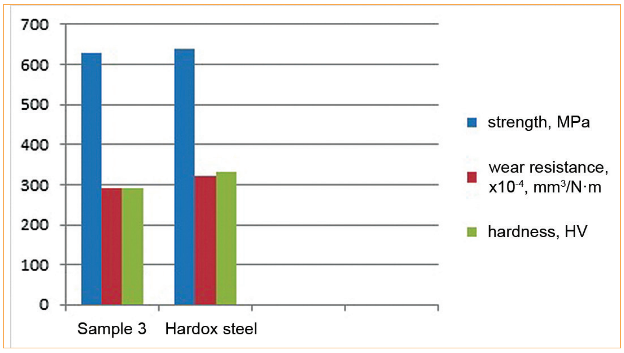

Fig. 5. Comparative diagram of properties of the pilot alloy and steel

The above-mentioned interstitial phases also are characterized by high hardness and strength, their presence in FCC solution matrix corresponds to an optimal structure of wear-resistant materials according to Charpy principle: a matrix with relative ductility and strength, with homogeneously distributed high-dispersion solid interstitial phase.

So, the revealed optimal niobium content for achievement of strength and ductility complex is approximately equal and makes 14—16 %, despite divergence in the structures noted in the researches [19—23] and in this research.

Comparative diagram of properties of the pilot alloy 3 (15.5 %) with the properties of Hardox 600 steel is presented in the **Fig. 5**. This grade was chosen for comparison, because it is widely used for manufacture of components operating in wear conditions. It can be seen from this diagram, that the properties of the alloy 3 are comparable with the properties of Hardox 600 steel, what can make possible its partial replacement in the prospect. Hardox steel is not manufactured in Kazakhstan, thereby the alloys, which were examined in this research can be competitive for Hardox steel, especially because self-produced charge materials were used for smelting of these alloys.

Conclusion

1. Partial use of ferroalloys in charge composition allows to obtain alloys of the Cr–Mn–Ni–Fe–Co–Nb system of the QHEA type that have a higher commercial attractiveness due to simplification of the smelting technology and the cost of the charge.

2. Introduction of niobium in the Cr–Mn–Ni–Fe–Co–Nb system in the amount of 14–16 % leads to increase of hardness, compression strength and wear resistance. The niobium content above 18 % leads to a slight decrease of these parameters, which can be explained by its uneven distribution in the structure.

3. For the experimental alloys of the Cr–Mn–Ni–Fe–Co–Nb system, obtained under the specified smelting conditions and charge composition, the Laves phase and the σ phase were not detected. Structure of the examined alloys is presented by FCC solid solution; it includes all metals with niobium content varying in a wide range. Additionally, the structure is presented by interstitial phases: carbide of $NbC_{0.76-1.0}$ type, manganese carbide of Mn_7C_3 type and intermetallic of CrNi type with cubic lattice.

4. Hardness, strength and wear resistance of the alloy 3 (with niobium content approximately 15 %) are comparable with the corresponding properties of Hardox 600 steel, what can make possible use of this alloy after additional technological improvement for manufacture of components operating in the conditions of abrasive wear.

The research was carried out within the framework of implementation of the Program BR21882240 "Developing a quasi high-entropy alloy using Kazakhstani raw materials and technology of producing precision parts based on it" (agreement with the Committee of Science of the Ministry of Education and Science of the Republic of Kazakhstan No. 378-PTsF-23-25 dated November 15, 2023), funded by the Ministry of Science and Higher Education of the Republic of Kazakhstan.

REFERENCES

1. Cantor B., Chang I. T. H., Knight P., Vincent A. J. B. Microstructural development in equiatomic multicomponent alloys. *Materials Science and Engineering: A*. 2004. Vol. 375–377. pp. 213–218.
2. Yeh J.-W. Recent Progress in High Entropy Alloys. *Ann. Chim. Sci. Mat*. 2006. Vol. 31. pp. 633-648.
3. Yeh J.-W., Chen S.-K., Lin S.-J., Gan J.-Y., Chin Ts.-Sh., Shun T.-Ts., Tsau Ch.-H., Chang Sh.-Y. Nanostructured High-Entropy Alloys with Multiple Principle Elements: Novel Alloy Design Concepts and Outcomes. *Advanced Engineering Materials*. 2004. Vol. 6. No. 8. pp. 299–303.
4. Ranganathan S. Alloyed pleasures: Multimetallic cocktails. *Curr. Sci.* 2003. Vol. 85. pp. 1404-1406.
5. Yeh J.-W., Chen Y.-L., Lin S.-J., Chen S.-K. High-entropy alloys – a new era of exploitation. *Mater. Sci. Forum*. 2007. 560. pp. 1–10.
6. Takeuchi A., Amiya K., Wada T., Yubuta K., Zhang W. High-entropy alloys with a hexagonal close-packed structure designed by equiatomic alloy strategy and binary phase diagrams. *JOM*. 2014. Vol. 66. pp. 1984–1992.
7. Zhang Y., Zuo T. T., Tang Z., Gao M. C., Dahmen K. A., Liaw P. K., Lu Z.P. Microstructures and properties of high-entropy alloys. *Prog. Mat. Sci.* 2014. Vol. 61. pp. 1–93.
8. Gali A., George E. P. Tensile properties of high and medium-entropy alloys. *Intermetallics*. 2013. Vol. 39. pp. 74–78. DOI: 10.1016/j.intermet.2013.03.018.7.
9. Ming-Hung Tsai, Jien-Wei Yeh. High-Entropy Alloys: A Critical Review. *Materials Research Letters*. 2014. Vol. 2. Iss. 3. pp. 107–123.
10. Ma X., Chen J., Wang X., Hu Y., Hue Y. Microstructure and mechanical properties of cold drawing Co–Cr–Fe–Mn–Ni high entropy alloy. *Journal of Alloys and Compounds*. 2019. Vol. 795. pp. 45–53. DOI: 10.1016/j.jallcom.2019.04.296.
11. Lin C.-M., Tsai H.-L. Effect of annealing treatment on microstructure and properties of high-entropy Fe–Co–Ni–Cr–$Cu_{0.5}$ alloy. *Mater. Chem. Phys*. 2011. 128. pp. 50–56.
12. Bataeva Z. B., Ruktuev A. A., Ivanov I. V., Yurgin A. B., Bataev I. A. Review of studying alloys developed based on the entropy approach. *Metal processing (technology, equipment, tools)*. 2021. Vol. 23. No. 2. pp. 116–146. DOI: 10.17212/1994-6309-2021-23.2-116-146.
13. Tung C. C., Yeh J. W., Shun T. T., Chen S.-K., Huang Y.-S., Chen H.-C. On the elemental effect of Al–Co–Cr–Cu–Fe–Ni high-entropy alloy system. *Materials Letters*. 2007. Vol. 61 (1). pp. 1–5. DOI: 10.1016/j.matlet.2006.03.140.
14. Tong C.-J., Chen M.-R., Chen S.-K., Yeh J.-W., Shun T.-T., Lin S.-J., Chang S.-Y. Mechanical performance of the Alx–Co–Cr–Cu–Fe–Ni high-entropy alloy system with multiprincipal elements. *Metall. Mater. Trans*. A. 2005. 36A. pp. 1263–1271.
15. Salishchev G. A., Tikhonovsky M. A., Shaysultanov D. G., Stepanov N. D., Kuznetsov A. V., Kolodiy I. V., Tortika A. S., Senkov O. N. Effect of Mn and V on structure and mechanical properties of high-entropy alloys based on Co–Cr–Fe–Ni system. *J. Alloy. Compd*. 2014. 591. pp. 11–21.
16. Yuhua Chen, Wenkuo Liu, Hongwei Wang et al. Effect of Ti Content on the Microstructure and Properties of Co–Cr–Fe–Ni–Mn–Ti High Entropy Alloy. *Entropy*. 2022. No. 2 (24). p. 241.
17. Ivchenko V. G., Pushin V. G., Uksusnikov A. N. Features of microstructure of cast high-entropy equiatomic alloys Al–Cr–Fe–Co–Ni–Cu. *Fizika metallov i metallovedenie*. 2013. Vol. 114. No. 6. p. 561.
18. Zhang H., Wang H., Liu Y. Improved strength and ductility in a Co–Cr–Fe–Ni–Mo high-entropy alloy system. *Journal of Alloys and Compounds*. 2014, 586. 478-483.
19. Bazlov A., Strochko I., Ubyivovk E., Parkhomenko M., Magomedova D., Zanaeva E. Structure and Properties of Amorphous Quasi-High-Entropy Fe–Co–Ni–Cr–(Mo,V)–B Alloys with Various Boron Content. *Metals*. 2023. Vol. 13. p. 1464. DOI: 10.3390/met13081464.
20. Zhihua Zeng, Mengqi Xiang, Dan Zhanga, Junjie Shi, Wei Wang, Xiaopeng Tang, Wenxiang Tang, Ye Wang, Xiaodong Ma, Zhiyuan Chen, Wenhui Ma, Kazuki Morita. Mechanical properties of Cantor alloys driven by additional elements: a review. *J. of Materials Research and Technology*. 2021. Vol. 15. pp.1920–1934. DOI: 10.1016/j.jmrt.2021.09.019.
21. Jiang Hui, Jiang Li, Qiao Dongxu, Lu Yiping, Wang Tongmin, Cao Zhiqiang, Li Tingju. Effect of Niobium on Microstructure and Properties of the Co–Cr–Fe–Nb–Ni High Entropy Alloys. *J. Mater. Sci. Technol*. 2017. Vol. 33 (7). pp. 712–717.
22. Zhang Jingyu, Xiong Ke, Huang Lin, Xie Bo, Ren Daping, Tang Chen, Feng Wei. Effect of Doping with Different Nb Contents on the Properties of Co–Cr–Fe–Ni High-Entropy Alloys. *Materials*. 2023. DOI: 16.6407.10.3390/ma16196407.
23. Průša F., Cabibbo M., Šenková A., Kučera V., Veselka Z., Školáková A., Vojtěch D., Cibulková J., Čapek J. High-strength ultrafine-grained Co–Cr–Fe–Ni–Nb high-entropy alloy prepared by mechanical alloying: Properties and strengthening mechanism. *Journal of Alloys and Compounds*. 2020. 835. 155308.
24. Zhaotong Li, Cainian Jing, Yan Feng, Zhonglin Wu, Tao Lin, Jingrui Zhao. Microstructure evolution and properties of laser cladding Nb containing eutectic high entropy alloys. *International Journal of Refractory Metals and Hard Materials*. 2023. 110. 105992.
25. Jixu Hu, Danyang Lin, Xingyi Li, Haolong Li, Jianguo Li, Zhengxin Tang, Xin Xi, Xiaoguo Song, Wei Fu. Interfacial strengthening mechanism of C/C/Nb0.74CoCrFeNi2/Nb brazed joints: Stress-relieving effects of the FCC phase. *Materials Science and Engineering*: A. 2022. 854. 143895.
26. Yang L., Li Y., Wang Z., Zhao W., Qin C. Nanoporous Quasi-High-Entropy Alloy Microspheres. *Metals*. 2019. Vol. 9. p. 345. DOI: 10.3390/met9030345.